Antiferromagnetic correlation effects in the metal-insulator crossover of the perovskite-type $La_{1-x}Sr_xTiO_3$ system



1998 J. Phys.: Condens. Matter 10 1003

(http://iopscience.iop.org/0953-8984/10/5/010)

J. Phys.: Condens. Matter **10** (1998) 1003–1011. Printed in the UK PII: S0953-8984(98)85235-1

# Antiferromagnetic correlation effects in the metal–insulator crossover of the perovskite-type $La_{1-x}Sr_xTiO_3$ system

Masashige Onoda and Masaki Kohno

Institute of Physics, University of Tsukuba, Tennodai, Tsukuba 305, Japan

Received 20 June 1997, in final form 8 October 1997

**Abstract.** The metal–insulator crossover of the perovskite-type $La_{1-x}Sr_xTiO_3$ system near $x = 0$ has been explored through measurements of the x-ray diffraction, electrical resistivity, thermoelectric power, Hall effect, and magnetization. This system ranges from being a highly correlated metal phase for $x > 0.05$ to being an antiferromagnetic metal-like phase for $0.01 \leqslant x \leqslant 0.05$ and then to being a variable-range hopping-like insulator phase for the composition $LaTiO_3$ with a bandwidth comparable to the electron correlation. The phase for $x \leqslant 0.05$ may be characterized in terms of local electron correlations as well as antiferromagnetic spin fluctuations.

## 1. Introduction

Metal–insulator transitions, hereafter referred to as MITs, in 3d-transition-metal ternary oxide systems have recently been investigated intensively in order to clarify the anomalous properties of correlated electrons [1, 2]. One of the most prototypical systems is the perovskite-type one with the chemical formula $MTO_3$, where M is an alkaline- or rare-earth element and T is a transition metal element such as Ti or V. In this system, the electron concentration and/or bandwidth can be controlled by the partial substitution of M ions. However, since MITs have often been accompanied by a structural distortion, it is not easy to clarify the driving force for the transition.

On the basis of transport, magnetic, thermal, and spectroscopic measurements for the $La_{1-x}Sr_xTiO_3$ system [2–14], it has been considered that $LaTiO_3$ is a Mott–Hubbard insulator, and that the compounds with concentrations in the range $x > 0.05$ are located in a highly correlated metal phase, in which the carrier mass increases critically with a constant Wilson ratio as the composition $LaTiO_3$ is approached [2, 8–12]. The transport properties of $RTiO_3$ (R = La, Ce, Pr or Nd) depend on the inhomogeneity of the atomic concentration and/or the comparability of the electron correlation $U$ and the bandwidth $W$ [14]: oxygen-deficient La and the nearly stoichiometric Ce compounds are like variable-range hopping (VRH) insulators with a finite density of states at the Fermi level $E_F$, while the compounds with excess oxygen (or cation deficiency) are highly or weakly correlated metals whose behaviour depends on their magnitudes of $W$ as well as random potentials. The existence of a pseudogap in the density of states for the highly correlated metals has also been suggested [14].

Systematic investigations of the $Ce_{1-x}Sr_xTiO_3$ and $CeTiO_{3+y/2}$ systems, where $0 \leqslant x \leqslant 1$ and $-0.36 \leqslant y \leqslant 0.44$, have revealed that for the crossover from correlated metals for $0.04 \leqslant x \leqslant 0.4$ to VRH-like insulators for $x < 0.02$, the system is accompanied by a

0953-8984/98/051003+09$19.50  

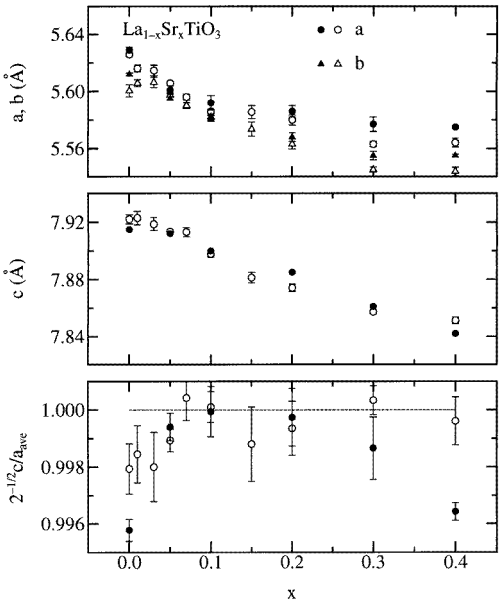


**Figure 1.** The $x$-dependences of the lattice constants and the lattice constant ratio $2^{-1/2}c/a_{\mathrm{ave}}$ for $La_{1-x}Sr_xTiO_3$, where $a_{\mathrm{ave}}$ is an average of $a$ and $b$: open symbols, this work; full symbols, after reference [6].

Jahn–Teller effect, a band dispersion anomaly, and canted magnetism for $x \leqslant 0.1$ [15]. The variations of the properties of $CeTiO_{3+y/2}$ with $y$ are rather similar to those of $Ce_{1-x}Sr_xTiO_3$ with $x$. Thus, not only a carrier mass enhancement but also the antiferromagnetic correlation effect have been considered to contribute to the metallic state near the boundary between the VRH-like insulators and metals.

It is expected that $La_{1-x}Sr_xTiO_3$ also experiences similar antiferromagnetic correlation effects to those that occur in $Ce_{1-x}Sr_xTiO_3$ and $CeTiO_{3+y/2}$, because these systems have similar crystal structures. On the basis of our preliminary data for $La_{1-x}Sr_xTiO_3$, we have already pointed out that this expectation may well prove correct [15]. This paper describes a detailed experimental study for $La_{1-x}Sr_xTiO_3$ near $x = 0$ through measurements of the x-ray diffraction, electrical resistivity, thermoelectric power, Hall effect, and magnetization. Section 2 describes the experimental methods, and section 3 presents the experimental results, referring appropriately to previous analysis procedures [14, 15]. Section 4 presents a unified discussion on the structural, transport, and magnetic properties clarified by this work, and section 5 is devoted to conclusions.

## 2. Experiments

Polycrystalline specimens of $LaTiO_3$ were prepared according to the same procedure as described in reference [14], and those of $SrTiO_3$ were obtained by the solid-state reaction method in air with $TiO_2$ (99.9% purity) and $SrCO_3$ (99% purity) at 1373 K for 12 hours. From an appropriate mixture of $LaTiO_3$ and $SrTiO_3$, the specimens of $La_{1-x}Sr_xTiO_3$ with $0 \leqslant x \leqslant 0.4$ were prepared finally with an Ar arc furnace. Electron-probe microanalysis (EPMA) was performed to estimate the cation concentration ratio.

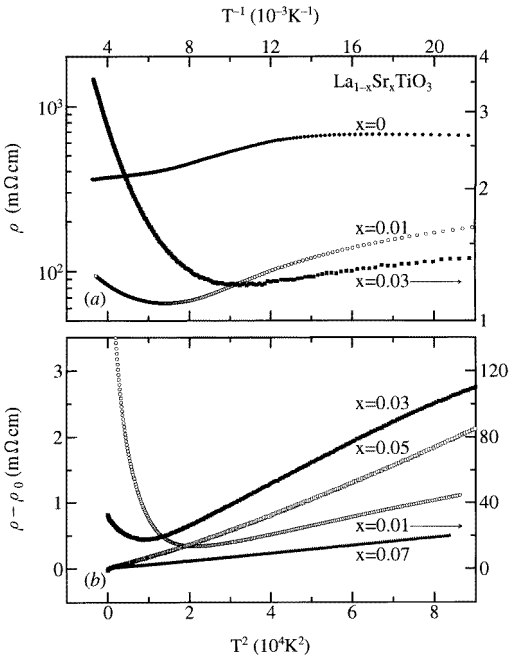


**Figure 2.** The temperature dependence of the electrical resistivity $\rho$ of $La_{1-x}Sr_xTiO_3$; (*a*) $\log\rho$ against $T^{-1}$ for $0 \leqslant x \leqslant 0.03$ and (*b*) $\rho - \rho_0$ against $T^2$ for $0.01 \leqslant x \leqslant 0.07$, $\rho_0$ being the residual resistivity.

X-ray powder diffraction patterns were obtained with Cu K$\alpha$ radiation at 290 K by a two-circle diffractometer. The four-terminal electrical resistivity and the thermoelectric power were measured by a DC method between 4.2 and 300 K. The Hall coefficient was measured at 290 K using a field of up to 15 kOe. The magnetization was obtained by the Faraday method with an applied field of up to 10 kOe between 4.2 and 1000 K, and the magnetic susceptibility was determined from the linear coefficient of the magnetization versus field ($M$–$H$) curve with a decreasing field.

## 3. Results

### *3.1. Lattice constants and the cation ratio*

The cation concentration ratio estimated by EPMA is nearly the same as the nominal value. Thus, the following discussion treats the nominal composition as that of the compound.

The powder diffraction patterns for all of the specimens indicate a single phase with an orthorhombic symmetry. The lattice constants $a$, $b$, and $c$ are shown as functions of $x$ in figure 1. The full symbols in this figure represent previous data [6]. They are consistent with our results for the range of $x \leqslant 0.2$, but a significant difference arises for $x > 0.2$. The cause of this discrepancy is not clear. The lattice constants are *not* linear in $x$; i.e. a simple Vegard rule is not valid for this system, which contrasts with the results for the spinel-type $Li_xMg_{1-x}V_2O_4$ system, which exhibits an Anderson-type MIT at $x \simeq 0.4$ [16]. The lattice constant ratio $2^{-1/2}c/a_{ave}$, where $a_{ave}$ is the average of the $a$- and $b$-values, plotted against $x$ at the bottom of figure 1, deviates significantly from unity for $x \leqslant 0.05$,

while for $x > 0.05$, it is nearly unity. This may indicate that for $x \leqslant 0.05$, a d electron occupies the $d_{xy}$ orbital due to the Jahn–Teller distortion [17] which is consistent with the results of structure analysis of $LaTiO_3$ [3, 6], but for $x > 0.05$ it occupies the degenerate orbitals.

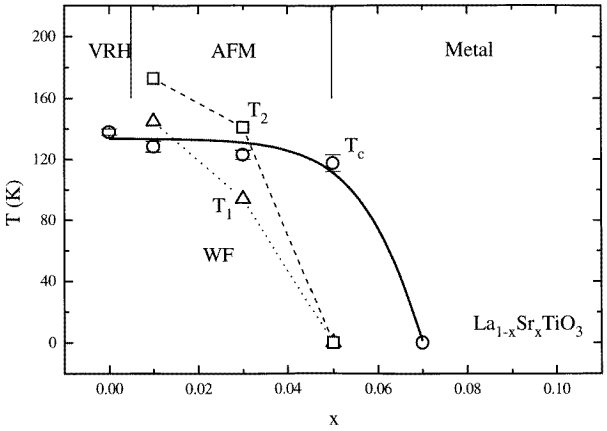


**Figure 3.** The phase diagram of $La_{1-x}Sr_xTiO_3$ with $0 \leqslant x \leqslant 0.1$: ○, magnetic transition temperatures $T_c$; △, temperatures $T_1$ above which $d\rho/dT$ is positive; □, temperatures $T_2$ above which $\rho$ has a $T^2$-dependence. 'Metal' indicates the highly correlated metal phase; 'AFM' indicates the antiferromagnetic metal-like phase; 'VRH' indicates the variable-range hopping-like insulator phase; 'WF' indicates the phase with canted magnetism. The full curve, and the dashed and dotted lines are drawn as guides to the eye.

### *3.2. Transport properties*

The electrical resistivity $\rho$ against the inverse temperature for $0 \leqslant x \leqslant 0.03$ is shown in figure 2(*a*). As previously reported [14], the conduction of $LaTiO_3$ at high temperatures is by hopping. On the other hand, at low temperatures, it is by means of extended states, although the temperature dependence does not follow a simple VRH conduction law; $\rho \propto \exp[(T_0/T)^{1/4}]$ with $T_0 = \alpha^3/D$, where $\alpha$ and $D$ represent the envelope of the wavefunction, as $\exp(-\alpha r)$, and the density of states for the hopping, respectively [18]. The resistivities for $x = 0.01$ and 0.03 are metallic above certain temperatures $T_1$ but, below $T_1$, they increase gradually with decreasing temperature. As shown in figure 2(*b*), the metallic resistivity for $x \geqslant 0.01$ approximately follows the relation $\rho - \rho_0 = AT^2$ over a certain temperature region above $T_2$, which may be one of the characteristics for a Fermi liquid [19], where the residual resistivities $\rho_0$ for $x = 0.01$, 0.03, 0.05, and 0.07 are 51, 0.77, 0.43, and 0.14 m$\Omega$ cm, respectively, and $A$ is a constant. Here, for $x = 0.05$, $A$ for the range $T > 170$ K appears to be larger than that for $T < 140$ K. While $\rho_0$ for $x \geqslant 0.1$ is nearly independent of $x$ [9], it appears to correlate with $A$ for $x < 0.1$. Figure 3 shows $T_1$ and $T_2$ against $x$ below $x = 0.07$, as open triangles and squares, respectively.

The temperature dependence of the thermoelectric power $S$ of $La_{1-x}Sr_xTiO_3$ is shown in figure 4. The positive thermoelectric power of $LaTiO_3$ suggests that a major contribution to the current lies below $E_F$. The result at low temperatures is characteristic for electron tunnelling between states at $E_F$, while at high temperatures, a dominant contribution to transport comes from hopping [14]. The data with $x = 0.01$ above 75 K are positive but, below this temperature, they are nearly zero. On the other hand, the data with $x \geqslant 0.03$

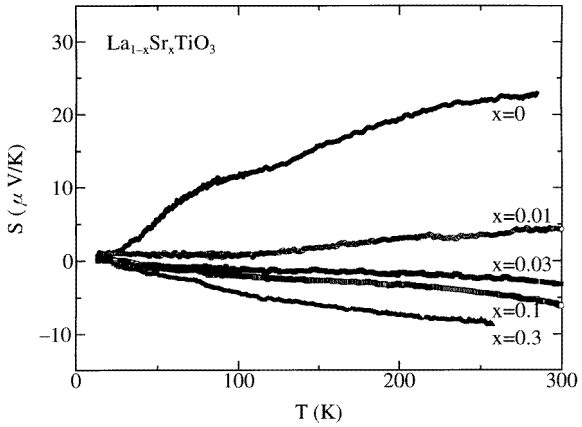


**Figure 4.** The temperature dependence of the thermoelectric power $S$ of $La_{1-x}Sr_xTiO_3$.

are negative, suggesting an electron carrier. The thermoelectric power for this $x$-region is approximately linear in temperature. By assuming that the effective mass $m_{\rm eff}$ is twice the free-electron mass and that the carrier density $n$ follows the free-electron relationship $n_{\rm free} \simeq 1.6 \times 10^{22}(1-x)$, the experimental results for $x > 0.05$ are roughly explained by the relation $S \simeq -(3e)^{-1}\pi^2 kT/E_{\rm F}$, where $k$ is the Boltzmann constant [20]. However, it is known that, in this $x$-region, the $m_{\rm eff}$-values estimated from the magnetization measurements significantly depend on $x$ [9]. Therefore, it is necessary to obtain a precise expression for the thermoelectric power on the basis of the actual band structure.

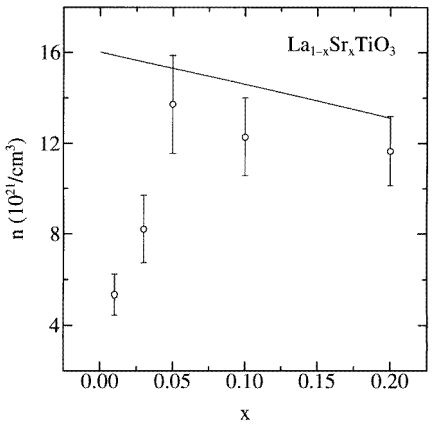


**Figure 5.** The $x$-dependence of the apparent carrier density $n$ of $La_{1-x}Sr_xTiO_3$ estimated from the Hall coefficient with a one-band model, where the full line shows the carrier concentration calculated from a free-electron relationship.

The Hall coefficients of $La_{1-x}Sr_xTiO_3$ at 290 K for $x \geqslant 0.01$ show a negative sign, suggesting an electron carrier. The *apparent* carrier concentration $n$ estimated from a one-band model is shown as a function of $x$ in figure 5. The full line shows the carrier concentration $n_{\rm free}$ defined above. For $x \geqslant 0.05$, $n$ agrees roughly with $n_{\rm free}$ [9] but, for $x = 0.01$ and 0.03, $n$ is significantly smaller than $n_{\rm free}$.

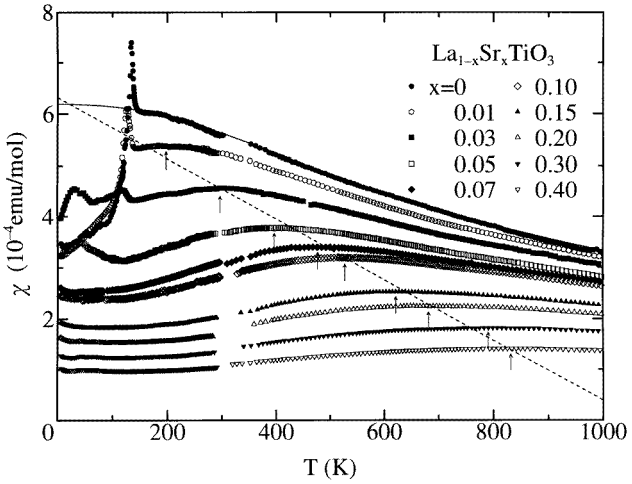


**Figure 6.** The temperature dependence of the magnetic susceptibility $\chi$ of $La_{1-x}Sr_xTiO_3$, where the full curve for $LaTiO_3$ shows the calculated Pauli paramagnetic susceptibility, the arrows indicate the positions of the susceptibility maxima, and the dotted line is drawn as a guide to the eye.

### *3.3. Magnetic properties*

The temperature dependence of the magnetic susceptibility $\chi$ of $La_{1-x}Sr_xTiO_3$ is shown in figure 6. Here, the $x$-dependence of the susceptibility at room temperature is fairly consistent with previous data for $x \geqslant 0.05$ [9]. For $x \leqslant 0.05$, a susceptibility peak or upturn at low temperatures exists, which may be related to the occurrence of a remanent magnetization basically due to an antisymmetric interaction as will be described later. The data for the paramagnetic region of $LaTiO_3$ have apparently been explained in terms of the free-electron model with $E_F = 984(5)$ K and the constant paramagnetism $\chi_0 = 2 \times 10^{-5}$ emu mol$^{-1}$ as shown by the full curve, because, in this compound, there is a finite density of states at $E_F$ [14] and $U/W \simeq 1$ [21]. The susceptibility for the paramagnetic region, where $x \geqslant 0.01$, has a broad peak at $T^*$, which is marked by the arrows in figure 6. $T^*$ increases with increasing $x$ and has a tendency to saturate at large $x$. From the viewpoint of the band theory, the part of the bandwidth with a width of about $kT$ around $E_F$ is responsible for the susceptibility at $T$. Thus, the present results indicate that the density of states at $E_F$ has a pseudogap as has been already pointed out for the highly correlated metal phase of La compounds with excess oxygen [14], and $E_F$ approaches a valley in the density of states as $x$ increases. Unfortunately, it is difficult to estimate the actual band form from the present data alone.

The remanent magnetization $\sigma$ defined as $M = \chi H + \sigma$ for $LaTiO_3$ is due to the antisymmetric interaction between the $Ti^{3+}$ ions [3, 14]. This appears for $x \leqslant 0.05$ [11]. The temperature dependence of $\sigma$ is shown in figure 7, and the transition temperature $T_c$ is plotted in figure 3 as the open circles. With increasing $x$, $\sigma$ decreases rapidly, but the decrease in $T_c$ is small. The data for $x = 0$ and 0.01 are explained approximately in terms of the relation $\sigma/\sigma_0 = \tanh[\sigma T_c/(\sigma_0 T)]$, where $\sigma_0$ is the value at 0 K [14]. From the full curves in figure 7, $J_{anis}/J$ or $\sigma_0/\mu_B$, where $J$ and $J_{anis}$ are the isotropic and anisotropic exchange constants, respectively, and $\mu_B$ is the Bohr magneton, is $9.3 \times 10^{-3}$ for $x = 0$ and $7.1 \times 10^{-3}$ for $x = 0.01$ [22, 23]. A slight discrepancy between the full curve and the

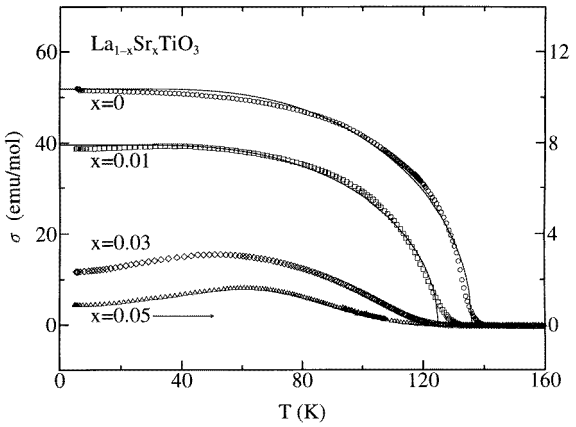


**Figure 7.** The temperature dependence of the remanent magnetization $\sigma$ of $La_{1-x}Sr_xTiO_3$, where the full curves for $x = 0$ and 0.01 indicate the calculated results.

data at around $T_c$ may be due to short-range-ordered effects. This result may indicate that the density of states at $E_F$ below $T_c$ is reduced due to the magnetic transition or band-gap formation, although it is still finite [14]. The data for $x = 0.03$ and 0.05 have a maximum at temperatures below $T_c$, which cannot be explained using the above relation.

## 4. Discussion

The properties of $La_{1-x}Sr_xTiO_3$ clarified by this work are summarized as follows.

(i) The Jahn–Teller distortion may lead to occupation of the $d_{xy}$ orbital for $x \leqslant 0.05$; outside this range the ground-state orbitals are degenerate.

(ii) For the electrical resistivity of the compounds with $x = 0.01$ and 0.03, the relation $\rho = \rho_0 + AT^2$ is still valid above certain temperatures.

(iii) The thermoelectric power is positive for $x \leqslant 0.01$; outside this range it is negative and varies linearly with temperature.

(iv) The Hall coefficient has a negative sign for $x = 0.01$ and 0.03, and the apparent carrier concentration with a one-band model is smaller than the value derived from the free-electron relationship.

(v) Except $LaTiO_3$, the compounds have a pseudogap in the density of states at $E_F$.

(vi) The temperature dependence of the remanent magnetization for $x = 0.03$ and 0.05 is different from that for $x = 0$ and 0.01.

For $x > 0.05$, the electronic state is considered to be basically a highly correlated Fermi liquid [2, 8–12, 24]. However, it should be noted that for $0.01 \leqslant x \leqslant 0.1$, the enhancement of $A$ is much stronger than that of $\chi^2$. This appears to be inconsistent with the usual Fermi liquid theory, in which $A$ and $\chi$ are expected to be proportional to $m_{\mathrm{eff}}^2$ and $m_{\mathrm{eff}}$, respectively [19]. Thus, an increase in $A$ through an antiferromagnetic correlation may also be expected for $x \leqslant 0.1$, and in particular for $x \leqslant 0.05$ as described below.

For $x = 0.05$, the compound is metallic over the whole temperature range, though remanent magnetization appears below $T_c$. The band gap that originates from the magnetic transition may be very small. This transition seems to be correlated with the change in $A$: i.e., $A$ for temperatures below $T_c$ is slightly smaller than that for temperatures above $T_c$.

For $x \leqslant 0.05$, $A$ is expected to increase significantly due to the greater strength of the antiferromagnetic instability. These properties suggest that the compound is roughly similar to an antiferromagnetic metal.

The compound with $x = 0.03$, where the bandwidth may be reduced due to a significant Jahn–Teller distortion, is still metallic above $T_c$, while below $T_c$, $d\rho/dT$ is negative. Since the thermoelectric power indicates that there is a finite density of states at $E_F$, the band gap due to the magnetic transition should still be small. The difference between $n$ and $n_{free}$ above $T_c$ indicates an anomaly in the band dispersion. Thus, an antiferromagnetic semimetal model is inferred to be applicable, in which the current should be carried by electrons and holes. The anomalous temperature dependence of the remanent magnetization for $x = 0.03$ and 0.05 has to be explained not in terms of a localized electron model but in terms of a band theory.

The results for $x = 0.01$ may be interpreted as indicating a crossover between the antiferromagnetic semimetal-like phase for $x = 0.03$ and the VRH-like insulator phase for the composition $LaTiO_3$. Here, there exists a discrepancy between the signs for carriers obtained from the thermoelectric power and Hall coefficient measurements. If the two-band model described above is applied, this discrepancy may be explained by considering the conductivity weight and the band form for each carrier.

These considerations provide the phase diagram shown in figure 3. Here, 'Metal' for $x > 0.05$ indicates the highly correlated metal phase with a small degree of antiferromagnetic correlation in the magnetic properties; 'AFM' for $0.01 \leqslant x \leqslant 0.05$ denotes the antiferromagnetic metal-like phase; 'VRH' for $LaTiO_3$ indicates the variable-range hopping-like insulator phase; 'WF' indicates the phase with canted magnetism. The existence of the antiferromagnetic metal phase located near the Mott–Hubbard insulator has been predicted qualitatively [1, 21]. For example, Mott has postulated a degenerate gas of spin polarons, in which a carrier tends to orient the moments of neighbouring atoms antiparallel to its own spin [1]. To achieve a quantitative understanding, further experimental and theoretical investigations are necessary. The VRH-like phase is different from the pure antiferromagnetic insulator phase that has been discussed theoretically, because the density of states at $E_F$ is finite and the susceptibility above the magnetic transition temperature is of the Pauli type as indicated by the comparability of $U$ and $W$ [14].

## 5. Conclusions

Through measurements of the lattice constant, electrical resistivity, thermoelectric power, Hall coefficient, and magnetization, this work has revealed that $La_{1-x}Sr_xTiO_3$ with $0 \leqslant x \leqslant 0.4$ undergoes successive transitions from the highly correlated metal phase for $x > 0.05$ to the antiferromagnetic metal-like phase for $0.01 \leqslant x \leqslant 0.05$ and then to the variable-range hopping-like insulator phase for the composition $LaTiO_3$. The latter transition may be closely related to the Mott–Hubbard-type one that appears as a band-crossing transition. For the highly correlated metal phase, the bandwidth may be controlled by the $GdFeO_3$-type distortion, while for the antiferromagnetic metal-like and variable-range hopping-like insulator phases, it may be reduced due to the Jahn–Teller distortion.

The phase for $x \leqslant 0.05$ should be described in terms of local electron correlations as well as antiferromagnetic spin fluctuations. Here, an electron–phonon interaction through the Jahn–Teller distortion may be also significant due to the carrier mass enhancement. Since the correlation effect and the electron–phonon interaction do not compete with each other, it is difficult to determine quantitatively the driving force for the transition from the highly correlated metal phase to the antiferromagnetic metal-like phase. The electronic

states of $La_{1-x}Sr_xTiO_3$ where $x \leqslant 0.05$ are comparable with those of $Ce_{1-x}Sr_xTiO_3$ and $CeTiO_{3+y/2}$ where $x, y \leqslant 0.1$ [15].

## Acknowledgment

We thank T Yamashita for his help in our experiments.

## References

[1] For a review, see
Mott N F 1990 *Metal–Insulator Transitions* 2nd edn (London: Taylor & Francis)
[2] For a review, see
Georges A, Kotliar G, Krauth W and Rozenberg M J 1996 *Rev. Mod. Phys.* **68** 13
[3] Eitel M and Greedan J E 1986 *J. Less-Common Met.* **116** 95 and references therein
[4] Lichtenberg F, Widmer D, Bednorz J G, Williams T and Reller A 1991 *Z. Phys.* B **82** 211
[5] Crandles D A, Timusk T and Greedan J E 1991 *Phys. Rev.* B **44** 13 250
[6] Sunstrom J E IV, Kauzlarich S M and Klavins P 1992 *Chem. Mater.* **4** 346
[7] Fujimori A, Hase I, Nakamura M, Namatame H, Fujishima Y, Tokura Y, Abbate M, de Groot F M F, Czyzyk M T, Fuggle J C, Strebel O, Lopez F, Domke M and Kaindl G 1992 *Phys. Rev.* B **46** 9841
[8] Fujishima Y, Tokura Y, Arima T and Uchida S 1992 *Phys. Rev.* B **46** 11 167
[9] Tokura Y, Taguchi Y, Okada Y, Fujishima Y, Arima T, Kumagai K and Iye Y 1993 *Phys. Rev. Lett.* **70** 2126
[10] Kumagai K, Suzuki T, Taguchi Y, Okada Y, Fujishima Y and Tokura Y 1993 *Phys. Rev.* B **48** 7636
[11] Okada Y, Arima T, Tokura Y, Murayama C and Môri N 1993 *Phys. Rev.* B **48** 9677
[12] Katsufuji T and Tokura Y 1994 *Phys. Rev.* B **50** 2704
[13] Crandles D A, Timusk T, Garrett J D and Greedan J E 1994 *Phys. Rev.* B **49** 16 207
[14] Onoda M and Yasumoto M 1997 *J. Phys.: Condens. Matter* **9** 3861
[15] Onoda M and Yasumoto M 1997 *J. Phys.: Condens. Matter* **9** 5623
[16] Onoda M, Imai H, Amako Y and Nagasawa H 1997 *Phys. Rev.* B **56** 3760
[17] Goodenough J B 1971 *Prog. Solid State Chem.* **5** 145
[18] Brenig W, Döhler G H and Wölfle P 1973 *Z. Phys.* **258** 381
[19] Kadowaki K and Woods S B 1986 *Solid State Commun.* **58** 507
[20] Wilson A H 1958 *The Theory of Metals* 2nd edn (London: Cambridge University Press)
[21] Moriya T 1985 *Spin Fluctuations in Itinerant Electron Magnetism* (Berlin: Springer)
[22] Dzyaloshinsky I 1958 *J. Phys. Chem. Solids* **4** 241
[23] Moriya T 1960 *Phys. Rev.* **120** 91
[24] Brinkman W F and Rice T M 1970 *Phys. Rev.* B **2** 4302